Postflight Data-Reduction Techniques for Hovered Kinetic Energy Weapons

Minjea Tahk* and Tom Trikas†
Integrated Systems Inc., Santa Clara, California 95054
and
Bryan Wallace‡
USAF Astronautics Laboratory, Edwards Air Force Base, California 93523

One of the major concerns in attitude control of kinetic-energy-weapon vehicles proposed for exoatmospheric engagements is that error sources such as vehicle center-of-gravity variations and thrust misalignments of divert thrusters may induce excessive parasitic torques on the vehicle. These torques may result in significant attitude perturbations that are undesirable for target tracking, especially when using strapdown seekers. In an effort to identify and characterize these error sources in a quantitative way, it has been proposed to explicitly estimate them by using the data obtained from kinetic-energy-weapon hovered interceptor test flights. An estimation procedure based on extended Kalman filtering is developed for the postflight data reduction that includes the estimation of the center-of-gravity location and thrust misalignments. Some modifications to the basic extended Kalman filter algorithm are made to reduce the sensitivity of the estimator to uncertainties in divert thrust timing. The proposed estimation scheme is then used to process simulated flight data and actual test data. The data-reduction results are provided in this paper.

Nomenclature

a_x, a_y, a_z	= vehicle acceleration in inertial frame
a_1, a_2, a_3, a_4	= thrust levels of attitude-control thrusters
d_1, d_2, d_3, d_4	= thrust levels of divert thrusters
F_x, F_y, F_z	= external forces in body frame
I_x, I_y, I_z	= principle moments of inertia
M_x, M_y, M_z	= external moments in body frame
m	= vehicle mass
p, q, r	= body angular rates in body frame
R_{acs}	= moment arm of attitude-control thrusters for roll
R_{dvt}	= moment arm of divert thrusters for roll
$T_{11} - T_{33}$	= elements of transformation matrix T, inertial-to-body reference frames
v_x, v_y, v_z	= vehicle velocity in inertial frame
X_{acs}	= moment arm of attitude-control thrusters for pitch and yaw
x, y, z	= vehicle position in inertial frame
x_{cg}, y_{cg}, z_{cg}	= c.g. variation from nominal location in body frame
$\Delta\theta_1, \Delta\theta_3$	= thrust misalignments of divert thrusters 1 and 3 in pitch plane
$\Delta\phi_1, \Delta\phi_2, \Delta\phi_3, \Delta\phi_4$	= thrust misalignments of divert thrusters 1, 2, 3, and 4 in roll plane
$\Delta\psi_2, \Delta\psi_4$	= thrust misalignments of divert thrusters 2 and 4 in yaw plane
ϕ, θ, ψ	= Euler angles (roll, pitch, and yaw, respectively)
ϕ_{acs}	= angle between attitude-control thrust vectors and z axis (45 deg nominal)

Received July 19, 1989; presented as Paper 89-3372 at the AIAA Guidance, Navigation, and Control Conference, Boston, MA, Aug. 14-16, 1989; revision received May 30, 1990; accepted for publication June 1, 1990. This paper is declared a work of the U.S. Government and is not subject to copyright protection in the United States.

*Research Scientist, Advanced Systems Department; currently, Assistant Professor, Department of Aerospace Engineering, Korea Advanced Institute of Science and Technology, Seoul, Korea. Member AIAA.

†Research Scientist, Advanced Systems Division, 3260 Jay Street. Member AIAA.

‡Staff Engineer, Aerospace Vehicles Division. Member AIAA.

Introduction

THE kinetic-energy-weapon hovered interceptor test (KHIT) program is a program in which several kinetic-energy-weapon (KEW) vehicles are test flown in a hovering mode of operation. The purpose of these tests is twofold. First, they will provide information on and experience in systems integration as applied to kinetic-energy-weapons. Second, analysis of flight test data will provide engineering data on parameters that will be useful in characterizing kinetic-energy-weapon performance. Of principal interest in this analysis is the determination of the vehicle center-of-gravity (c.g.) and thruster misalignments since these significantly impact vehicle attitude control.

Typical kinetic-energy-weapon configurations utilize a set of thrusters, termed divert thrusters, that are mounted in a cruciform arrangement in the plane of the c.g. and provide the lateral maneuver capability required to ensure target intercept. An on-board infrared seeker is mounted on the vehicle in a strapdown configuration to provide guidance commands during the terminal phase of the target intercept. The strapdown configuration of the seeker requires that the vehicle modify its attitude to maintain the target image within the seeker field of view. However, if divert thruster misalignments and c.g. shifts are large, then significant attitude perturbations will result each time a divert thruster fires and may cause the vehicle to lose its lock on the target.

The c.g. location and thruster misalignments are not constant but instead vary as fuel is consumed during the flight and as the thruster nozzles and throats erode. Thruster ablation can change the thrust vector thus creating an effective thruster misalignment even if the thruster nozzle itself is perfectly aligned. Thus, even though the magnitude of these parameters can be determined from manufacturing specifications, direct experimentation is essential to verify that c.g. location and thrust misalignments remain within tolerable ranges throughout the flight.

This paper describes the procedure developed for estimation of c.g. position and divert thruster misalignments from test flights. This procedure is based on an extended Kalman filter (EKF)[1] with some modifications to tailor it to the test data-reduction requirements. Specifically, an adaptive estimation scheme is used to handle the difficulties in estimation caused

by uncertain timing of divert thrust pulses. Inputs to this estimator consist of angular rate and translational acceleration measurements provided by an onboard inertial reference unit (IRU) and the known thruster-valve commands (both attitude and divert). This paper also describes the method used for the validation of the estimation software. Some numerical results showing the impact of structural vibration on estimation accuracy are provided. Finally, the results of the data reduction based on actual flight test data are presented to demonstrate the performance of the estimation scheme.

Test Vehicle Configuration

The basic configuration of the flight test vehicle is shown in Fig. 1. A body-fixed coordinate system with the x axis pointing along the vehicle roll axis, the z axis pointing downward, and the y axis chosen so as to form a right-handed coordinate system has been defined here to simplify further discussions. Also, divert and attitude thrusters have been numbered to allow for easy reference.

Translational accelerations commanded by the control system are generated by four bipropellant divert thrusters each of which generates 350-lbf thrust nominal at sea level. These are mounted in a cruciform arrangement and placed so that they act through the nominal design c.g. Since there are no thrusters pointing along the x axis, there is no direct control over the vehicle's longitudinal motion. Instead, the vehicle's pitch angle is altered so that firing of divert thruster 1 generates accelerations in the longitudinal direction. In a similar manner, the vehicle's roll angle can be altered to generate lateral accelerations.

Attitude control of the vehicle is accomplished through the use of four bipropellant attitude-control thrusters each generating 8-lbf thrust nominal at sea level and mounted in a bow-tie configuration at the aft end of the vehicle. By firing the appropriate pairs of thrusters, the required vehicle torques can be generated. Since only four thrusters are being used, attitude control about each of the roll, pitch, and yaw channels is coupled and a suitable thruster distribution law must be used.

Onboard instrumentation consists principally of a strapdown IRU containing three rate gyros and three accelerometers. The IRU outputs incremental changes in velocities and attitudes at a rate of 100 Hz. The control strategy used in the hover test vehicle is to relay onboard IRU measurements to the ground via a telemetry link. A ground computer then computes control commands for the divert thruster and attitude-control thrusters in terms of thruster-valve commands. These are then uplinked to the vehicle and used to control thruster firing. Both divert and attitude control are implemented using "bang-bang" control logic. Attitude-thruster commands consist of on/off signals updated at 100 Hz, whereas divert-thruster commands are updated at 20 Hz intervals.

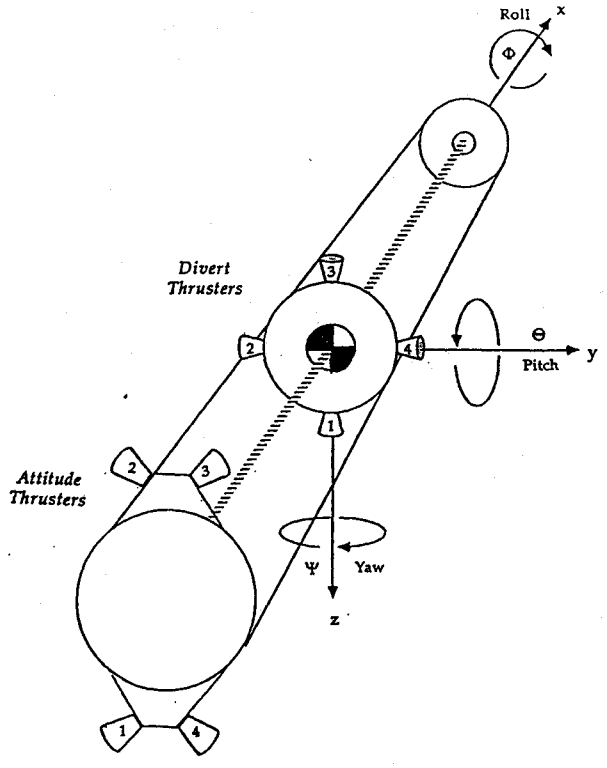

Fig. 1 Flight test vehicle geometry. Four ACS thruster configuration.

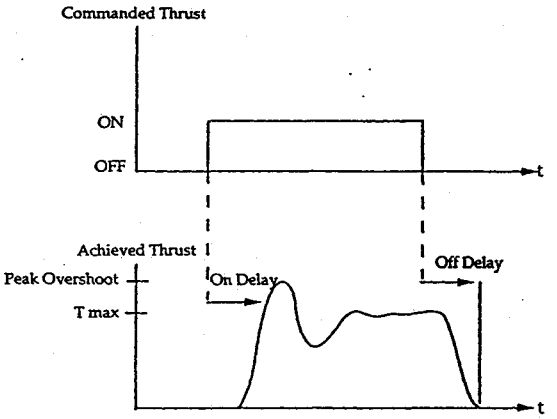

Fig. 2 Commanded thrust and typical achieved thrust profile.

Test Vehicle Dynamic Model

In order to develop an algorithm for the estimation of the desired parameters, a dynamic model that fully represents the true dynamics of the test vehicle is required. The inclusion of minor details of dynamics in this model, however, will not necessarily improve estimation accuracy while increasing computational burden. A good example of this is the inclusion of a structural model of the test vehicle in the estimation algorithm. Thus, even though the proposed data processing is an off-line algorithm, some simplifications of the vehicle dynamics must be made to keep the computational burden to an acceptable level.

In this study, the following assumptions are applied to the development of the vehicle dynamic model.

1) Test vehicle has only rigid-body dynamics.

2) Thrust misalignments and c.g. offsets can be modeled by random walk processes. (Since there is no a priori information available, c.g. motion and thruster misalignments are assumed to be random-walk phenomena which are obtained simply by integrating white noise.)

3) Sensor errors contain only uncorrelated random noise.

4) Sensor location errors and misalignments are insignificant.

5) Attitude-thruster misalignments are negligible.

6) Divert thrusters do not produce moments if there are no c.g. offsets and thrust misalignments.

Although only divert thruster 1 will be fired during initial hover testing, the dynamic model presented here includes the effects of all four divert thrusters. The differential equations governing the dynamics are then as follows:

$$\dot{x} = v_x, \quad \dot{y} = v_y, \quad \dot{z} = v_z$$

$$\dot{v}_x = (T_{11}F_x + T_{21}F_y + T_{31}F_z)/m + \xi_{vx}$$

$$\dot{v}_y = (T_{12}F_x + T_{22}F_y + T_{32}F_z)/m + \xi_{vy}$$

$$\dot{v}_z = (T_{13}F_x + T_{23}F_y + T_{33}F_z)/m + g + \xi_{vz}$$

$$\dot{\phi} = p + q\sin\phi\tan\theta + r\cos\phi\tan\theta$$

$$\dot{\theta} = q\cos\phi - r\sin\phi$$

$$\dot{\psi} = q\sin\phi/\cos\theta + r\cos\phi/\cos\theta$$

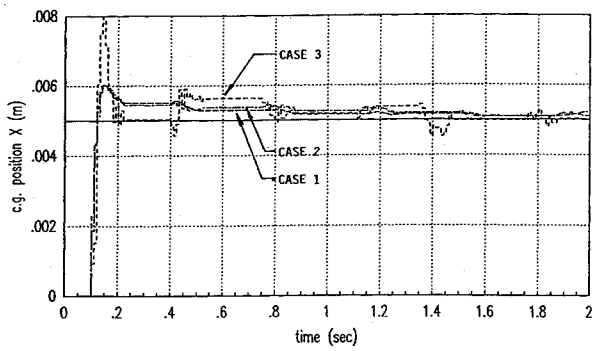

Fig. 3 The x_{cg} estimated from simulated data.

$$
\begin{aligned}
\dot{p} &= [M_x + (I_y - I_z)qr]/I_x + \xi_p \\
\dot{q} &= [M_y + (I_z - I_x)rp]/I_y + \xi_q \\
\dot{r} &= [M_z + (I_x - I_y)pq]/I_z + \xi_r \\
\dot{x}_{cg} &= \xi_{xcg}, \quad \dot{y}_{cg} = \xi_{ycg}, \quad \dot{z}_{cg} = \xi_{zcg} \\
\Delta\dot{\theta}_1 &= \xi_{tm1}, \quad \Delta\dot{\psi}_2 = \xi_{tm2}, \quad \Delta\dot{\theta}_3 = \xi_{tm3}, \quad \Delta\dot{\psi}_4 = \xi_{tm4} \\
\Delta\dot{\phi}_1 &= \xi_{tm5}, \quad \Delta\dot{\phi}_2 = \xi_{tm6}, \quad \Delta\dot{\phi}_3 = \xi_{tm7}, \quad \Delta\dot{\phi}_4 = \xi_{tm8}
\end{aligned}
$$

where $\xi_{(\cdot)}$ denote zero-mean white Gaussian noise. The transformation matrix T from the inertial frame to the body frame is computed as follows:

$$
T = \begin{bmatrix}
\cos\psi\cos\theta & \sin\psi\cos\theta & -\sin\theta \\
-\sin\psi\cos\phi + \cos\psi\sin\theta\sin\phi & \cos\psi\cos\phi + \sin\psi\sin\theta\sin\phi & \cos\theta\sin\phi \\
\sin\psi\sin\phi + \cos\psi\sin\theta\cos\phi & -\cos\psi\sin\phi + \sin\psi\sin\theta\cos\phi & \cos\theta\cos\phi
\end{bmatrix}
$$

The external forces and moments acting on the vehicle are also computed as

$$
\begin{aligned}
F_x &= -d_1\Delta\theta_1 - d_2\Delta\psi_2 + d_3\Delta\theta_3 + d_4\Delta\psi_4 \\
F_y &= d_2 - d_4 + (a_1 + a_2 - a_3 - a_4)\sin\phi_{acs} + d_1\Delta\phi_1 - d_3\Delta\phi_3 \\
F_z &= -d_1 + d_3 + (-a_1 + a_2 + a_3 - a_4)\cos\phi_{acs} + d_2\Delta\phi_2 - d_4\Delta\phi_4 \\
M_x &= R_{acs}(-a_1 + a_2 - a_3 + a_4) - y_{cg}F_z + z_{cg}F_y \\
&\quad - R_{dvt}(d_1\Delta\phi_1 + d_2\Delta\phi_2 + d_3\Delta\phi_3 + d_4\Delta\phi_4) \\
M_y &= X_{acs}(-a_1 + a_2 + a_3 - a_4)\cos\phi_{acs} - z_{cg}F_x + x_{cg}F_z \\
&\quad - R_{dvt}(d_1\Delta\theta_1 + d_3\Delta\theta_3) \\
M_z &= X_{acs}(-a_1 - a_2 + a_3 + a_4)\sin\phi_{acs} - x_{cg}F_y + y_{cg}F_x \\
&\quad - R_{dvt}(d_2\Delta\psi_2 + d_4\Delta\psi_4)
\end{aligned}
$$

In these equations, the vehicle mass and moments of inertia are not estimated but assumed to be known since the estimation of these variables from flight test data is not technically feasible. In actual flight tests, measurements of mass and moments of inertia made before and after each test are used to predict the time histories of mass and moments during flight. In general, the mass of the vehicle m, can be modeled as

$$
m(t) = m_0 - \frac{I_{t,d}}{gI_{sp,d}} - \frac{I_{t,a}}{gI_{sp,a}}
$$

where m_0 is the initial mass and $I_{t,d}$ and $I_{t,a}$ are total impulses produced by the divert thrusters and attitude-control thrusters up to the current time t, respectively, and $I_{sp,d}$ and $I_{sp,a}$ are associated specific impulses. Thus, the vehicle mass is computed from

$$
\dot{m} = -\frac{d_1 + d_2 + d_3 + d_4}{gI_{sp,d}} - \frac{a_1 + a_2 + a_3 + a_4}{gI_{sp,a}}
$$

where the thrust levels are predicted from valve commands and the specific impulses may be determined from static test data. If the final mass is measured, the values of the specific impulses can be calibrated using the measured mass reduction and the total impulse computed from the valve commands. The dynamics of the moments of inertia, I_x, I_y, and I_z, are complicated by the internal motion of propellant. However, some relationships between the changes of the moments of inertia and $\dot{m}$ may be derived as follows:

1) If we assume that the vehicle is a cylinder of a uniform mass distribution, then the moments of inertia are given as

$$
I_x = \frac{1}{8}mD^2, \qquad I_y = \frac{1}{12}mL^2, \qquad I_z = \frac{1}{12}mL^2
$$

where D and L are the diameter and length of the vehicle, respectively. Hence, knowledge of the current mass of the vehicle will allow determination of its moments of inertia. In practice, however, the above relations are not directly applicable since the initial and final values of the moments of inertia cannot be precisely matched with the true values that are available from direct measurements.

2) An alternative, preferred approach is to assume that mass flow rate and the rate of change of moment of inertia are linearly related, i.e.,

$$
\dot{I}_x = K_x\dot{m}, \qquad \dot{I}_y = K_y\dot{m}, \qquad \dot{I}_z = K_z\dot{m}
$$

where $K_{(\cdot)}$ are the proportionality constants. From the measurements of the initial and final mass and moments of inertia, these proportionality constants can be computed as

$$
K = \frac{I_{\text{initial}} - I_{\text{final}}}{m_{\text{initial}} - m_{\text{final}}}
$$

Data Reduction Based on Extended Kalman Filter

The algorithm used to process the flight test data is based on an EKF, a description of which can be found in any standard text on estimation theory (e.g., Ref. 1, pp. 188).

Linearization of the nonlinear state and measurement matrices are computed numerically using the central-difference method. Although analytical expressions for these linearized matrices can be derived for computational efficiency, numerical differentiation is advantageous since algorithm and code development time can be significantly reduced.

In this section, technical difficulties associated with data reduction are discussed, and an adaptive filter switching scheme adopted for the data reduction is described. Finally, observability issues related to the estimation of vehicle position, velocity, attitude, and c.g. location are discussed.

State Variables to be Estimated

The measurements available from hover tests are IRU outputs and valve commands. IRU outputs consist of three rate components and three acceleration components sampled at

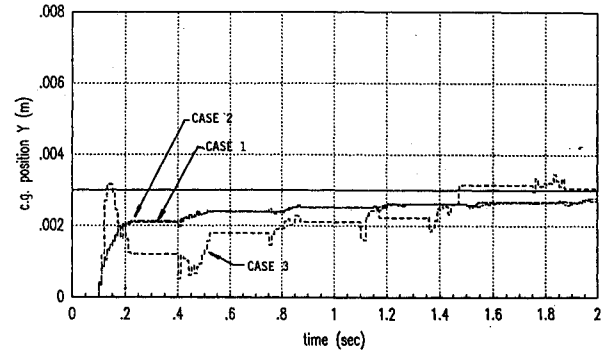

Fig. 4 The y_{cg} estimated from simulated data.

100 Hz. Valve commands from the guidance computer are also sampled at 100 Hz. No explicit measurements of vehicle position and attitude are made. Without these measurements, vehicle position, velocity, and attitude are not observable. Instead, these variables are computed by integrating the vehicle dynamics.

Since the thrust misalignments of a divert thruster are only observable when that particular thruster is on and the current test vehicle is equipped with only one divert thruster (no. 1), the thrust misalignments of the other divert thrusters (nos. 2, 3, and 4) are not estimated. For the same reason, the estimation of the thrust misalignments of divert thrust 1, $\Delta\theta_1$ and $\Delta\phi_1$, is expected to be terminated when divert thruster 1 is off. However, it has been observed that the EKF is still active even after the thruster is turned off. This is because, while the thruster is on, the filter observes some correlation between the thruster misalignments and the other states such as body rates. This correlation is expressed in the corresponding off-diagonal terms of the covariance matrix P, which slowly decay when the thruster is turned off. Until these off-diagonal terms reduce to zero, the estimation of $\Delta\theta_1$ and $\Delta\phi_1$ remains active. Even though this transient altering activity is mathematically correct, it does not make sense physically because the thrust misalignments disappear as the thruster is turned off. Thus, the EKF algorithm is modified to stop the estimation of $\Delta\theta_1$ and $\Delta\phi_1$ and reset the corresponding off-diagonal elements of the covariance matrix P to zero upon the termination of each thrust pulse.

A similar problem to the one described above exists for the estimation of c.g. location. Rigorously speaking, the c.g. location is still observable without divert thrusters if attitude control thrusters are active. However, the expected c.g. shifts are so small compared to the moment arms of the attitude control thrusters and the uncertainties in attitude thrust levels that the c.g. location is effectively unobservable unless a divert thruster is firing. Furthermore, any c.g. variation along the z axis is unobservable since only divert thruster 1 is firing. To show this explicitly, consider the force and moment components produced by a misalignment in the pitch plane of $\Delta\theta_1$, which are given by

$$\begin{aligned}
\Delta F_x &= -d_1\Delta\theta_1 \\
\Delta F_y &= d_1\Delta\phi_1 \\
\Delta F_z &= 0 \\
\Delta M_x &= -y_{cg}F_z + R_{dvt}d_1\Delta\phi_1 \\
\Delta M_y &= x_{cg}F_z - R_{dvt}d_1\Delta\theta_1 \\
\Delta M_z &= 0
\end{aligned}$$

where only first-order effects of the error sources are retained. Since the contributions of z_{cg} are only second-order effects, the estimation of z_{cg} is not practically feasible.

As can be seen from the preceding expressions, the accuracy of acceleration measurements is important for the separation of the effects of c.g. shifts and thrust misalignments, although

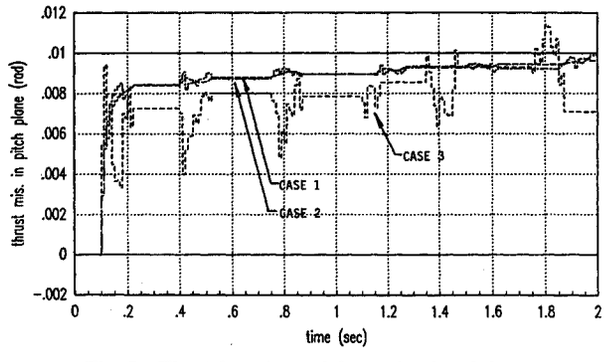

Fig. 5 The $\Delta\theta_1$ estimated from simulated data.

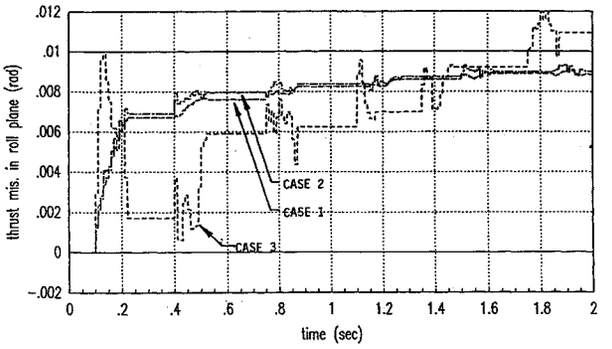

Fig. 6 The $\Delta\phi_1$ estimated from simulated data.

this separation is implicitly done by the EKF filter. If acceleration measurements are not reliable, the estimation accuracy of both c.g. shifts and thrust misalignments will be poor whatever the accuracy of rate measurements are.

Finally, we have to consider the estimation characteristics of the vehicle mass and moments of inertia. Basically, the mass and moments of inertia of the vehicle can be either directly estimated from the IRU outputs and valve commands or extrapolated from the initial values using the formulas described in the previous section. In earlier filter formulations,[2] the mass and moments of inertia were treated as state variables and explicitly estimated. Estimation accuracy, however, was not better than the accuracy that could be obtained from the methods described earlier. Poor mass estimation using the explicit scheme is attributed to the larger errors in predicting thrust ($\approx 5\%$),[3] as compared to the errors in characterizing thruster fuel consumption based on valve-command histories.

The explicit estimation of moments of inertia by using the EKF algorithm is also found to be impractical. In this case, uncertainties in predicting thrust are on the same order as the total change in moments of inertia from wet-to-dry vehicle. Furthermore, since the IRU output rate is equal to the attitude-control thruster pulse width, it is very difficult to estimate angular accelerations, hence moments of inertia, especially in light of the small rotational motions induced during the hover test flight. In the current version of the EKF software, the moments of inertia are simply predicted from the mass-time history and the initial moments of inertia by using the derived proportionality constants K_x, K_y, and K_z.

In summary, the vehicle states that can be effectively estimated from the IRU outputs and valve commands are body rates (three states), c.g. offset (two states), and thrust misalignments (two states), or

$$X_{est} = [p,\ q,\ r,\ x_{cg},\ y_{cg},\ \Delta\theta_1,\ \Delta\phi_1]$$

where the error sources, x_{cg}, y_{cg}, $\Delta\theta_1$, and $\Delta\phi_1$, are only observable when divert thruster 1 is on.

Adaptive Estimation

It is obvious that successful estimation depends on the accuracy of the input and measurement data. Unfortunately, the actual thrust levels of divert and attitude thrusters are not known. Also, valve states that can be used to predict thrust levels are not well known either. Although extra information on actual valve states is available from an additional data link, difficulties in synchronization of IRU data with these valve state measurements reduce the usefulness of this information. Thus, the actual valve commands synchronized with IRU data are used as inputs to the vehicle dynamic model, which includes a thruster-valve dynamic model.

Thruster-valve commands can be related to the achieved thrust as is shown in Fig. 2. The dominant features here are the significant but unequal on and off delays and a thrust overshoot on startup. Note that even during steady-state burn, the thrust is not constant.

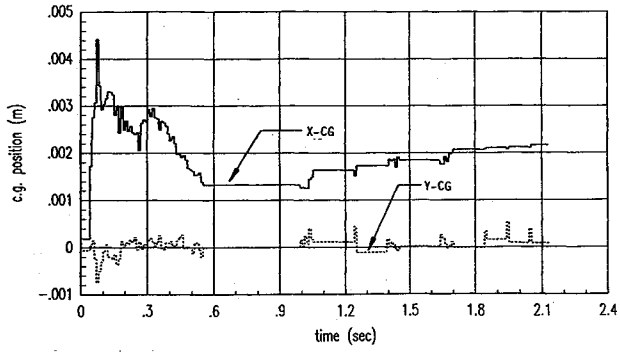

Fig. 7 The c.g. location estimated from flight test data.

Test data obtained from the static test of the thrusters show that the prediction of thrust levels from valve commands may not be satisfactory.[4,5] The time delay between valve commands and thrust exhibits significant variation both from pulse to pulse and from thruster to thruster. Uncertainties in thrust levels are also observed. To compensate for these variations, the use of additional state variables referred to as thrust scale factors is considered in Ref. 2. Although scale factors are useful for the tracing of variations in thrust levels, it is observed that any asynchronization of the predicted and true thrust levels causes large fluctuations in the estimated scale factors, rendering the whole estimation scheme unreliable. Numerical experiments show that the use of scale factors cannot even handle 5-ms time-delay errors. This timing problem cannot be solved by correlation with IRU acceleration measurements since the sample rate of 100 Hz is too slow to determine the exact timing of thrust rise and fall.

In this study, the thrust levels are simply computed from the valve commands using assumed time delays. The parameters such as thrust levels and time delays are determined by using the available static test data. An adaptive switching scheme is then employed to minimize the effects of the time-delay errors on the estimation accuracy. This scheme estimates divert thrust levels from two sources, divert thruster-valve commands and acceleration measurements, to determine whether the divert thrusters are turned on or off. If the two estimation values do not agree within a certain error bound, then it is declared that a time-delay error exists between the predicted thrust levels based on valve commands and true thrust levels. Then, the EKF is effectively turned off for the estimation of c.g. location and thrust misalignments so that the estimates are not contaminated by the time-delay errors. However, the estimation of the body rates continues.

When the filter is partially turned off, some adjustments are made to the covariance matrix of the state estimation error and the covariance matrix of the assumed process noise. First, the strength of the process noise associated with the c.g. location is reduced since the propellant consumption is low during the period that the divert thruster is off. This adjustment may not be applicable for thrust misalignments since a certain change of thrust vector is possible when a thruster is activated again. Also, if the c.g. locations and the thrust misalignments are not estimated, the off-diagonal terms of the error covariance matrix relating the c.g. location and thrust misalignments with other variables are not valid any more. Thus, these off-diagonal terms are reset to zero whenever divert thruster 1 is off.

Simulation Results

The vehicle model used in the estimation algorithm is a simplified one in which some of the detailed dynamic characteristics of the hover vehicle such as aerodynamics, structural vibration, products of inertia, sensor dynamics, and sensor quantization are absent. In order to test the sensitivities of the estimation algorithm to these unmodeled dynamics, simulated flight test data is generated by an independent six-degree-of-freedom simulation code that includes these details. For example, the following three simulations are made to study the effects of sensor quantization error and structural vibration on the estimation accuracy: case 1: no IRU noise or quantization, no structural vibration; case 2: quantization is only IRU error, no structural vibration; and case 3: IRU quantization, random noise, plus structural vibration. Parameter valves are assumed to be $x_{cg} = 0.005$ m; $y_{cg} = 0.003$ m; $\Delta\theta_1 = 0.01$ rad; and $\Delta\phi_1 = 0.01$ rad.

Case 1 is the ideal case but sensor dynamics still remain. The results of case 1 provide the upper bound of the estimator performance. Case 2 is included to study the effects of IRU quantization. Case 3 contains all possible IRU errors as well as structural vibration effects. The performance of the estimator in processing real test data may be predicted from the result of case 3.

The exact values of thrust levels, mass, and moments of inertia obtained from simulation are used in the data reduction in these examples. To account for the interval-averaging nature of IRU sensors, the IRU outputs are advanced by half the sample interval. Also, the time lags associated with IRU dynamics are treated as additional pure time delays in the estimation algorithm.

Figures 3 and 4 show the estimated x_{cg} and y_{cg}. Also, the estimated thrust misalignments $\Delta\theta_1$ and $\Delta\phi_1$ are shown in Figs. 5 and 6. It is shown that the impact of quantization errors on estimation accuracy is not significant. The estimation accuracy seems to be deteriorated by structural vibration, but the estimated values converge to the true ones. In this comparison study, the filter is tuned for case 3, and the same filter parameters are also used for the other cases.

Experimental Results

In this section, the estimation results based on the actual hover test data are presented. The test data are sampled at 100 Hz and last for 2.15 s. Since the true thrust levels are unknown, the valve dynamics of the simulation are used to predict valve position and thrust level for each thruster. Also, the vehicle mass and moments of inertia are independently computed according to the method described previously.

Time delays associated with IRU outputs are corrected by using the same method discussed in the previous section. Furthermore, the time delay associated with the divert thruster and attitude-control thrusters are approximately corrected by using average values obtained from static tests.

The estimated c.g. offsets and thrust misalignments are shown in Figs. 7 and 8, respectively. The variances of the estimation errors are also shown in Figs. 9 and 10. The fine tuning of filter parameters for actual test data is not possible since the true covariances of the estimation errors are unknown. However, it is found from the simulation results with various filter parameters that the value of the measurement noise variances that include the IRU noise and the structural vibration model are reasonable for the processing of the actual test data.

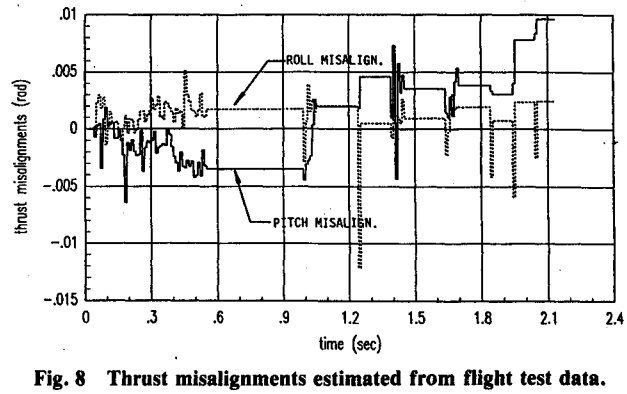

Fig. 8 Thrust misalignments estimated from flight test data.

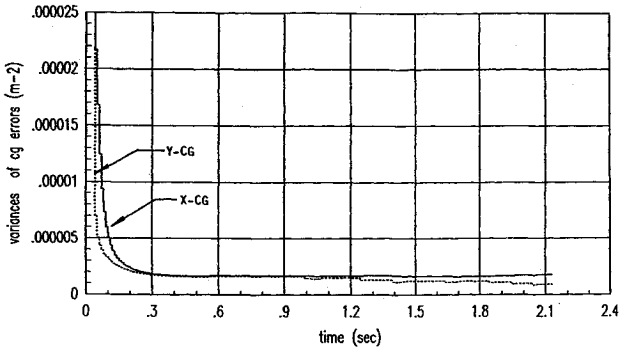

Fig. 9 Variances of c.g. estimation errors.

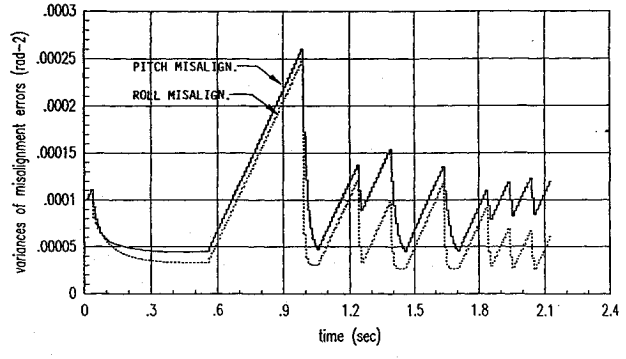

Fig. 10 Variances of thrust misalignment estimation errors.

It is observed in Figs. 7 and 8 that the state estimates tend to drift after the first second of the flight. These drift characteristics are believed to be caused by the diverging pitch angle experienced by the vehicle during flight. Since the pitch angle is not estimated explicitly but simply predicted by integrating body rates, the errors in computing the pitch angle from the body rates may be significant if the flight time is long or the body pitch rate is high. If the predicted missile attitude is not correct, then the computation of the gravity effects on accelerometers is not correct, inducing errors in the measurement equations of acceleration. It is also noted that the accuracy of acceleration measurements are essential in distinguishing the effects of c.g. shifts from those of thrust misalignments. Thus, if acceleration measurements are erroneous, both of the estimates for c.g. shifts and thrust misalignments are not reliable.

Attitude prediction performed by the ground computer for guidance/control may not be accurate enough to resolve the gravitational acceleration correctly. However, this problem can be easily solved if any reliable device is used to measure the missile attitude during the test. An alternative to avoid the difficulty associated with uncertain missile attitude is to process only rate measurements to estimate the disturbance torques that are the combined effects of c.g. shifts and thrust misalignments. This approach is immune to any accelerometer errors but does not allow for the discrimination of c.g. shifts and thrust misalignments. It is still useful, however, in that it allows the engineer to determine bounds on the divert induced-parasitic torques, hence accurately determine attitude-control requirements.

Conclusions

In this paper, the estimation techniques developed for the postflight data-reduction kinetic-energy-weapon hovered interceptor test data are described. Simulated and experimental results are presented. These results show that the techniques based on an extended Kalman filter adequately estimate the c.g. location and thrust misalignments. The adaptive estimation scheme is effective in reducing estimator sensitivity to uncertainties in predicting the divert thrust time history. The performance of the estimator with actual flight data is comparable to its performance with simulated data.

The proposed estimation scheme satisfies the data reduction requirements of kinetic-energy-weapon hovered interceptor test and yields information that is useful for comparison to theoretical predictions and in characterizing kinetic-energy-weapon performance in terms of c.g. migration and thruster misalignments. This is of significant benefit in the design of KEW control systems.

Acknowledgments

The first two authors would like to thank their co-workers at Integrated Systems Inc., Robert McEwen, for generating the simulation results, and Richard Bortins and M. Michael Briggs, for their helpful technical comments during the course of this study. Also, the authors gratefully acknowledge the support from Allan Weston of the U.S. Air Force Astronautics Laboratory, Edwards AFB, CA.

References

[1]Gelb, A., *Applied Optimal Estimation,* MIT Press, Cambridge, MA, 1974, Chap. 6.

[2]Barnhart, D., Weston, A., and Trikas, T., "KEW Propulsion System Performance Requirements," 1987 JANNAF Propulsion Meeting, San Diego, CA, Dec. 1987.

[3]Trikas, T., "Divert Thruster Test Data Analysis," Integrated Systems Inc., Rept. 123, Santa Clara, CA, April 1988.

[4]McEwen, R., "KHIT IMU Model," Integrated Systems Inc., Rept. 131, Santa Clara, CA, June 1988.